Molecular and Cellular Endocrinology xxx (2017) 1–14

Contents lists available at ScienceDirect

Molecular and Cellular Endocrinology

journal homepage: www.elsevier.com/locate/mce

Structural aspects of Vitamin D endocrinology

Natacha Rochel [a, *], Ferdinand Molnár [b, **]

[a] Institut de Génétique et de Biologie Moléculaire et Cellulaire (IGBMC), Institut National de La Santé et de La Recherche Médicale (INSERM), U964/Centre National de Recherche Scientifique (CNRS), UMR7104/Université de Strasbourg, 67404 Illkirch, France
[b] Institute of Biopharmacy, School of Pharmacy, Faculty of Heath Science, University of Eastern Finland, Yliopistonranta 1C, Canthia 2036, 70210 Kuopio, Finland

ARTICLE INFO

Article history:
Received 22 December 2016
Received in revised form
27 February 2017
Accepted 27 February 2017
Available online xxx

Keywords:
Vitamin D3
DBP
CYPs
VDR
HVDRR
Structure
Allostery

ABSTRACT

1α,25-Dihydroxvitamin D_3 ($1,25(OH)_2D_3$) is the hormonally active form of vitamin D_3. Its synthesis and its metabolites, their transport and elimination as well as action on transcriptional regulation involves the harmonic cooperation of diverse proteins with vitamin D binding capacities such as vitamin D binding protein (DBP), cytochrome P450 enzymes or the nuclear vitamin receptor (VDR). The genomic mechanism of $1,25(OH)_2D_3$ action involves its binding to VDR that functionally acts as a heterodimer with retinoid X receptor. The crystal structures of the most important proteins for vitamin D_3, VDR, DBP, CYP2R1 and CYP24A1, have provided identification of mechanisms of actions of these proteins and those mediating VDR-regulated transcription. This review will present the structural information on recognition of the vitamin D_3 and metabolites by CYP proteins and DBP as well as the structural basis of VDR activation by $1,25(OH)_2D_3$ and metabolites. Additionally, we will describe, the implications of the VDR mutants associated with hereditary vitamin D-resistant rickets (HVDRR) that display impaired function.

1. Introduction

The active form of vitamin D_3, 1α,25-Dihydroxyvitamin D_3 ($1,25(OH)_2D_3$), acts as an endocrine hormone and primarily maintains calcium levels in plasma and phosphate homeostasis. In addition to endocrine hormone actions, locally produced $1,25(OH)_2D_3$ displays paracrine/autocrine actions (Morris and Anderson, 2010) that are important for epidermal differentiation (Bikle *et al.*, 2004) or innate immune response (Liu *et al.*, 2006).

Vitamin D_3 can be obtained from dietary sources or is synthesized in the skin after sunlight exposure. The activation of vitamin D_3 is accomplished by sequential hydroxylations, 25-hydroxylation of vitamin D_3 leading to 25-hydroxyvitamin D_3, $25(OH)D_3$, followed by the 1α-hydroxylation (Fig. 1). The first step of 25-hydroxylation occurs in the liver (Ponchon and DeLuca, 1969), and the second one occurs both in the kidney and extra-renal sites (Fraser and Kodicek, 1970; Hewison and Adams, 2011). Several cytochrome P450 enzymes, such as CYP2R1, CYP27A1, CYP3A4, CYP2D25, are able to hydroxylate at C-25. The second hydroxylation at C-1α is done by CYP27B1 (Gray *et al.*, 1972).

Catabolic desactivation pathways include a carbon-24 oxidation by CYP24A1 leading to calcitroic acid production, and a 26,23-lactone pathway for converting both $25(OH)D_3$ and $1,25(OH)_2D_3$ to lactone products (Prosser and Jones, 2004). All of the CYPs that are involved in vitamin D hydroxylation, catalyze single or multiple hydroxylation reactions on specific carbons of the vitamin D_3 substrate using a transient heme-bound intermediate. All CYP proteins show high conservation and exhibit a common secondary structure with multiple highly conserved helices, A to L, connected by loops and β-sheet structures. Crystal structures of CYP2R1 (Strushkevich *et al.*, 2008) and CYP24A1 (Annalora *et al.*, 2010) provided insights into the vitamin D hydroxylation mechanism.

Vitamin D_3 metabolites including $1,25(OH)_2D_3$ are transported by a serum vitamin D binding protein (DBP), also known as GC-globulin (Daiger *et al.*, 1975). DBP also binds saturated and unsaturated fatty acids with moderate affinity, monomeric actin and is able to depolymerize filamentous actin. The crystal structures of DBP bound to $25(OH)D_3$ (Verboven *et al.*, 2002) as well as bound to actin (Otterbein *et al.*, 2002; Head *et al.*, 2002) were solved.

Most of the biological actions of $1,25(OH)_2D_3$ are achieved through Vitamin D Nuclear Receptor (VDR)-mediated regulation of

* Corresponding author.
** Corresponding author.
E-mail addresses: rochel@igbmc.fr (N. Rochel), ferdinandmolnar@gmail.com (F. Molnár).

http://dx.doi.org/10.1016/j.mce.2017.02.046
0303-7207/

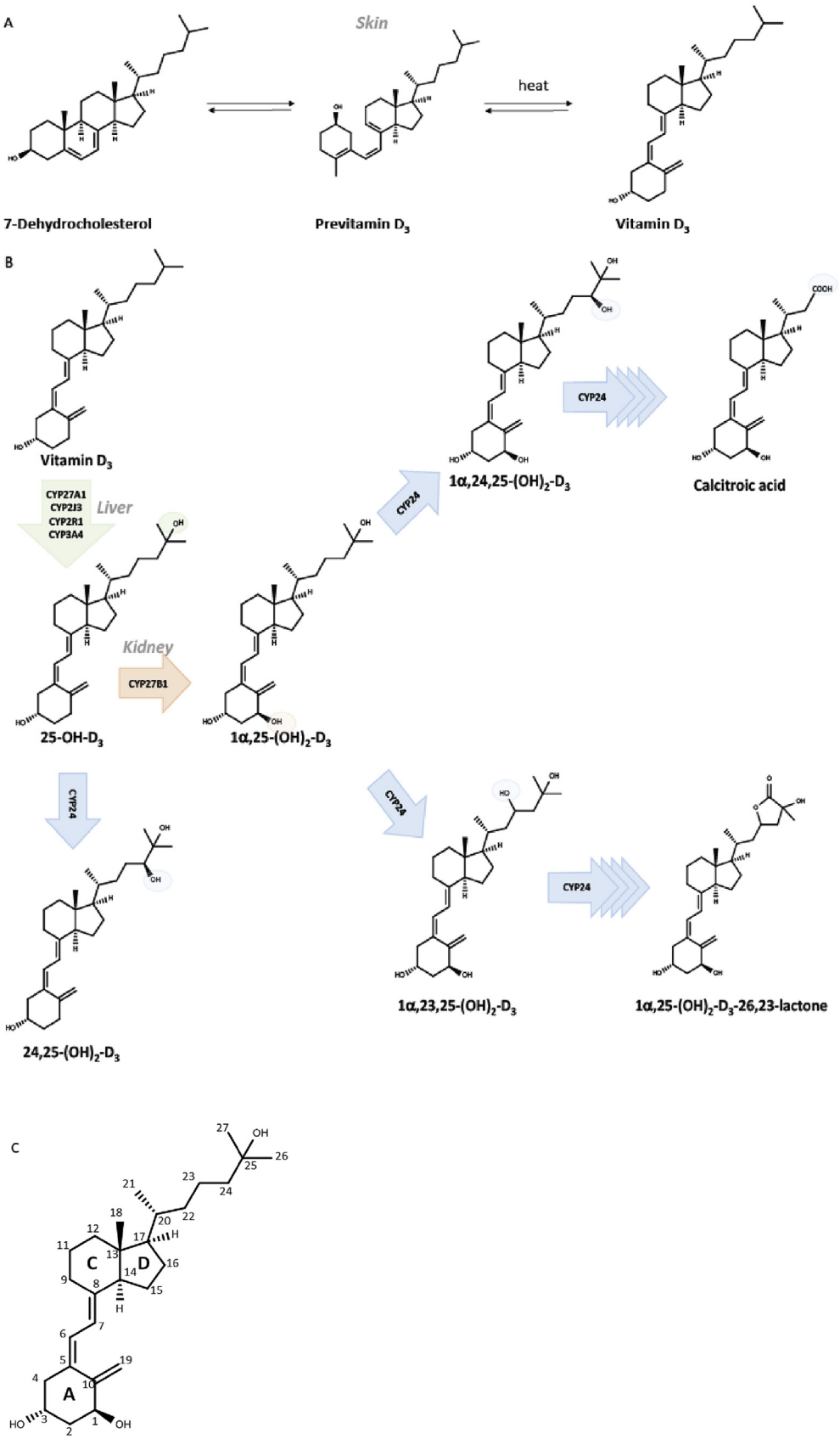

Fig. 1. (A–B) Vitamin D_3 synthesis, activation and inactivation. (C) Chemical structure and numbering of $1,25(OH)_2D_3$.

Please cite this article in press as: Rochel, N., Molnár, F., Structural aspects of Vitamin D endocrinology, Molecular and Cellular Endocrinology (2017), http://dx.doi.org/10.1016/j.mce.2017.02.046

gene expression. Among key genes that are regulated by $1,25(OH)_2D_3$ there are those controlling calcium transport, detoxification, transcription factors, immunomodulation, inflammation, oxidation, development and cancer-related, etc. (Pike, 2011; Haussler *et al.*, 2013; Carlberg, 2014).

The VDR (NR1I1) is a member of the nuclear receptor (NR) superfamily that classically acts as a heterodimer with one of the three retinoid X receptor (RXR) isotypes (RXRα, NR2B1; RXRβ, NR2B2; and RXRγ, NR2B3). VDR binds with high affinity $1,25(OH)_2D_3$. VDR is a promiscuous NR and its deregulation may lead to severe diseases such as cancers, psoriasis, rickets, renal osteodystrophy, and autoimmunity disorders (multiple sclerosis, rheumatoid arthritis, inflammatory bowel diseases, type I diabetes) (Bouillon *et al.*, 2006; Feldman *et al.*, 2014; Mangin *et al.*, 2014; Lin and Li, 2016).

VDR mediates the biological effects of its ligand by regulating the transcription through binding to specific DNA motif in the promoter of controlled target genes. In a ligand-dependent manner, the DNA-bound heterodimer recruits various coregulators of transcription: typically, in the absence of ligands or in the presence of antagonists, corepressors are recruited to the target genes, while agonist ligands induce a change in the structure of the NR that allows interaction with coactivators. Recruitment of coactivators results first in histone acetylation which prepares target gene promoters through decondensation of the chromatin and, further, in a link with the basal transcriptional machinery. Numerous proteins with large structural and functional diversities have been identified as VDR coregulators (Molnár, 2014).

VDR shares the main structural characteristics of NRs: it consists of a highly conserved DNA-binding domain (DBD), a ligand-binding domain (LBD), and a hinge region connecting the DBD to the LBD. Other NRs comprise also a variable N-terminal domain (NTD) displaying a ligand-independent activation function; however, the NTD domain of VDR is very short [23 AA in human VDR (hVDR)] and its function is not completely understood. The DBD contains two zinc fingers, each containing a zinc atom coordinated by four cysteine residues in a tetrahedral arrangement (Shaffer and Gewirth, 2002). The LBD of the NRs harbors a ligand-dependent activation function, or AF-2, a major interface for homo- and heterodimerization and an interface for coactivators as well as corepressors. The first crystal structure of hVDR LBD-$1,25(OH)_2D_3$ (Rochel *et al.*, 2000) revealed a similar fold as the other NRs. Because of the high pharmaceutical potential of VDR ligands, the mechanism of the receptor functioning has been intensively investigated, and structural details of the VDR signaling are now available for various VDR ligands [reviewed in (Molnár, 2014; Belorusova and Rochel, 2014; Yamada and Makishima, 2014)].

Hereditary vitamin D-resistant rickets (HVDRR) is a rare genetic disease caused by mutations in the VDR gene that result in the complete or partial loss of receptor functions, including DNA binding, heterodimerization with RXR, coregulators recruitment and ligand binding. Up to date, around 50 different mutations have been identified within the VDR [reviewed in (Feldman and Malloy, 2014)].

Here, we will discuss the structural information on recognition of the Vitamin D_3 and metabolites by CYP proteins and DBP as well as the structural basis of VDR activation by $1,25(OH)_2D_3$ and natural metabolites. We will primarily focus on structural data obtained by X-ray crystallography, but also will highlight allosteric insights of VDR function provided by other structural methods on integral proteins. Additionally, we will describe, based on structural knowledge, the VDR mutants associated with hereditary vitamin D-resistant rickets (HVDRR) that display impaired function.

2. Structures of CYPs in complex with vitamin D_3 and metabolites

2.1. CYP2R1 in complex with vitamin D_3

The first crystal structure of a CYP enzyme involved in vitamin D activation was CYP2R1 in complex with vitamin D_3 (PDB ID: 3C6G) (Strushkevich *et al.*, 2008). The CYP2R1 forms a homodimer in solution and crystallized as such linked by 2-hydroxypropyl-β-cyclodextrin detergent molecules. It has a typical P450 fold, consisting of 12 α-helices (A–L) with β-sheets mostly on one side and the heme buried deeply inside the protein (Fig. 2A). Helices E, I, J, K and L form the core of the protein. Helices F and G are involved in the homodimer interface and formation of the active site. The heme is tightly bound to CYP2R1 through hydrogen bonds of the D-ring propionate with Trp133, Arg137, Arg446 and the A-ring propionate

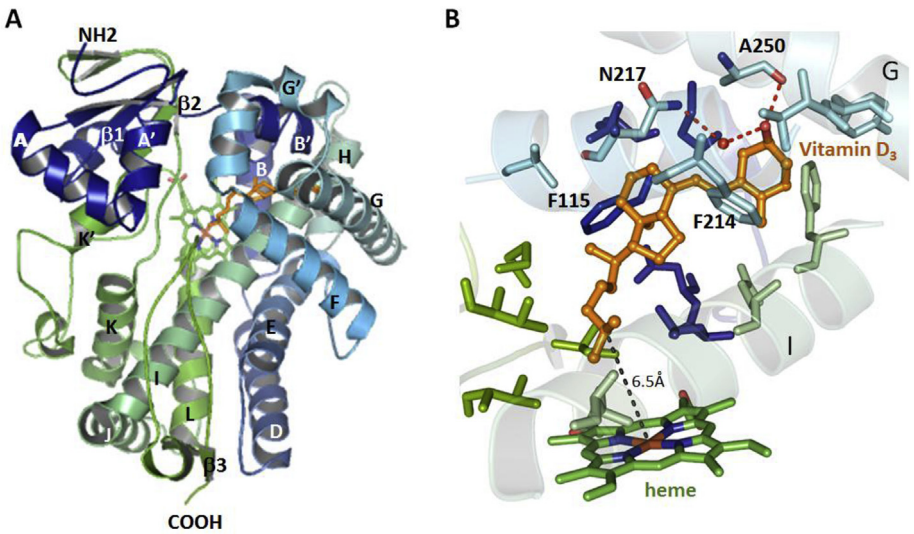

Fig. 2. CYP2R1-vitamin D_3 crystal structure. (A) Overall structure of human CYP2R1. The heme (in green) and vitamin D_3 (in orange) are shown in stick representation. (B) Close-up view of the binding of vitamin D_3 in the active site. Interacting residues are shown in stick representation. Hydrogen bonds formed by 3β-OH are shown as red dashed lines. Helices of the active site represented as transparent cartoon. Black dashed line indicates the distance between the C-25 carbon atom of vitamin D_3 from the heme.

Please cite this article in press as: Rochel, N., Molnár, F., Structural aspects of Vitamin D endocrinology, Molecular and Cellular Endocrinology (2017), http://dx.doi.org/10.1016/j.mce.2017.02.046

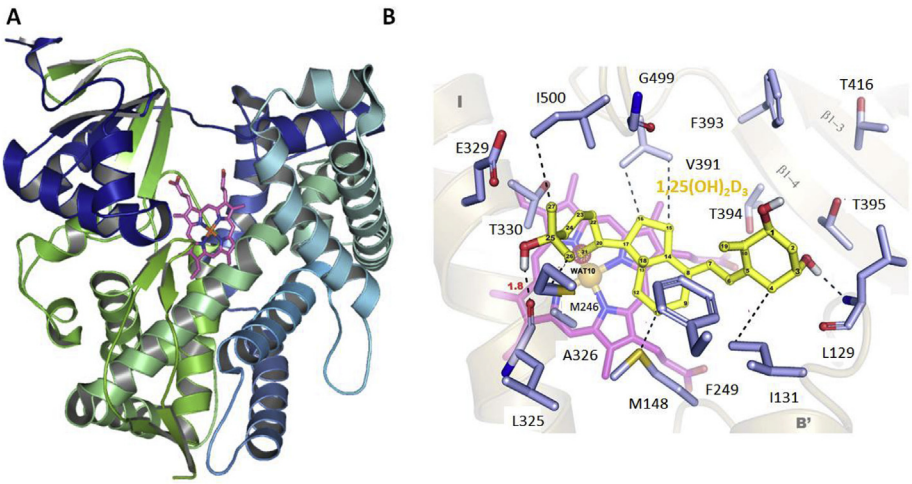

Fig. 3. CYP24A1 crystal structure. (A) Overall structure of human CYP24A1. The heme (in pink) is shown in stick representation. (B) Docking of $1,25(OH)_2D_3$ (yellow) binding in the heme-centered (pink) active site of CYP24A1 (adapted from Annalora *et al.*, 2010). Amino acid residues that flank the secosteroid docking site are shown in stick representation.

with Arg109, His381 and Ser442.

Vitamin D_3 in the CYP2R1 occupies a position between helices G and I and the B′ helix/B-C loop with the side chain pointing toward the heme group, in an elongated conformation (Fig. 2B). The residues lining the active site are mostly hydrophobic. The 3β-OH group of the A-ring is accessible from the surface of the protein. The A-ring adopts a chair conformation with an axial orientation of the 3β-OH group. The 3β-OH group of vitamin D_3 forms a hydrogen bond with the amide group of Ala250 of the helix G and a water-mediated hydrogen bond with Asn217 of the helix F. The A-ring is surrounded by aromatic side-chains residues. The conjugated triene of vitamin D_3 has a planar geometry perpendicular to the heme and forms van der Waals interactions with Phe214 of helix F. The C-18 methyl group of vitamin D_3 makes a hydrophobic contact with the aromatic side-chain of Phe115 of helix B'. The 17β-aliphatic side-chain of vitamin D_3 adopts a conformation that places C-25 toward the heme iron, for hydroxylation. However, the C-25 carbon atom of vitamin D_3 appears to be less optimally positioned for the hydroxylation at a distance of 6.5 Å from the heme iron in contrast to the optimal 4.9 Å distance observed in other CYP-substrate structure (PDB ID: 1R9O).

2.2. CYP24A1 crystal structures

The crystal structure of ratCYP24A1, involved into catabolic desactivation of $1,25(OH)_2D_3$, has been solved in the presence of the detergents Cymal and CHAPS (PDB IDs: 3K9V and 3K9Y) (Annalora *et al.*, 2010). The crystal asymmetric unit contains 2 molecules of CYP24A1. CYP24A1, initially referred to as the 25-hydroxyvitamin D_3 -24-hydroxylase, is able to catalyze multiple hydroxylation reactions at carbons C-24 and C-23 of the side chain of both $25(OH)D_3$ and its hormonal form, $1,25(OH)_2D_3$ in order to attenuate vitamin D signaling associated with calcium homeostasis and cellular growth processes. The 3D structure of CYP24A1 displays the canonical P450 fold, including the 12 α-helices (A–L) and four β-sheets (β1–β4), as well as additional helices and the conserved heme binding motif and a substrate-binding cavity (Fig. 3A). $1,25(OH)_2D_3$ docks (Fig. 3B) in the open form of CYP24A1 forming two hydrogen bonds, between the 3β-OH group with Leu129 and between the 25-OH group Leu325 (helix I) and multiple hydrophobic interactions as modelled

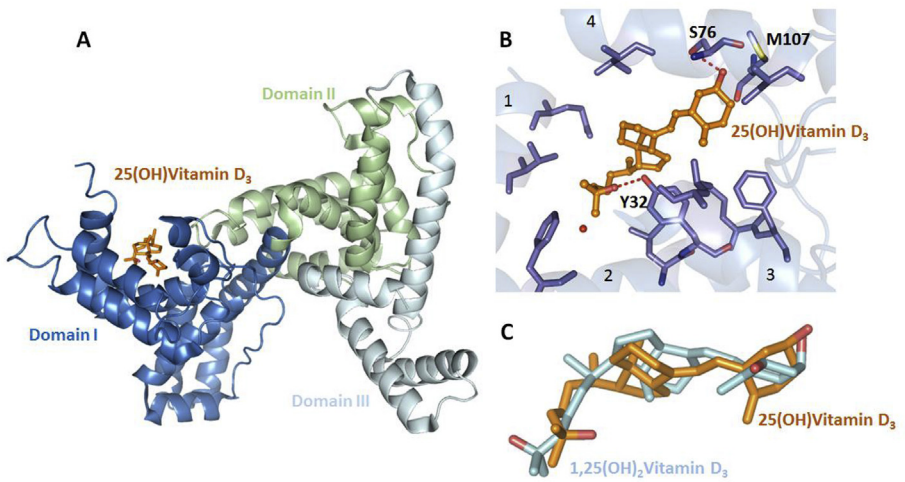

Fig. 4. DBP-$25(OH)D_3$ crystal structure. (A) Overall structure of DBP with the 3 different domains shown in different colors. The $25(OH)D_3$ is shown in tick representation in orange. (B) Close-up view of the binding of $25(OH)D_3$ in the active site of DBP. Interacting residues are shown in stick representation. Hydrogen bonds formed by the hydroxyl groups are shown as red dashed lines. Helices of the active site represented as transparent cartoon. (C) Conformations of $25(OH)D_3$ in DBP complex superposed to $1,25(OH)_2D_3$ in VDR complex.

Please cite this article in press as: Rochel, N., Molnár, F., Structural aspects of Vitamin D endocrinology, Molecular and Cellular Endocrinology (2017), http://dx.doi.org/10.1016/j.mce.2017.02.046

by Annalora *et al.*, 2010.

3. Crystal structure of DBP bound to 25(OH)D_3

DBP is the major carrier of vitamin D_3 and its metabolites, 25(OH)D_3 and 1,25(OH)$_2D_3$. DBP also binds monomeric actin (G-actin) and slowly depolymerizes filamentous actin. Human DBP has been crystallized in complex with 25(OH)D_3 (PDB ID: 1J78) (Verboven *et al.*, 2002). The asymmetric unit contains 2 molecules of DBP, one molecule bound to 25(OH)D_3 and one without. DBP is composed of three domains: domain 1 contains 10 α-helices, domain 2 is similar to domain 1 with a coil replacing helix 7 and domain 3 contains only 4 helices (Fig. 4A). The 25(OH)D_3 is bound in a cleft on the surface by residues of helices 1–6 of domain 1 (Fig. 4B). The ligand is bound by hydrophobic residues and hydrogen bonds between the 25-OH group with Tyr32 and between the 3-OH group and Ser76 and Met107. The weak density of the map around the ligand indicates some flexibility of the ligand. The β side of the C/D rings points to the solvent. Modeling of the 1,25(OH)$_2D_3$ indicates that th e 1α-OH group will induce a steric hindrance with Met107, thus explaining the lower affinity of DBP for 1,25(OH)$_2D_3$ compared to 25(OH)D_3. The A-ring adopts an A-chair conformation within DBP complex and different conformations of the triene and of the side chain (Fig. 4C) compared to 1,25(OH)$_2D_3$ bound to VDR (see below).

4. Recognition of 1,25(OH)$_2D_3$ by VDR LBD

4.1. Crystal structure of hVDR LBD in complex with 1,25(OH)$_2D_3$

Detailed information on the molecular mechanism of action of 1,25(OH)$_2D_3$ has been initially obtained by the elucidation of the crystal structure of its complex with the hVDR LBD (PDB ID: 1DB1) (Rochel *et al.*, 2000) that has revealed a conformation similar to other agonist-bound NR LBDs crystal structures. The general fold of VDR LBD consists of a three-layered α-helical sandwich composed of 12 helices (H1 to H12) and a three-stranded β-sheet (Fig. 5A). The ligand-binding pocket (LBP) is located on the bottom of the LBD and is surrounded by helices H2-3, H5-7, H10 and H12. The residues of each of β-sheet strands also form contacts with a ligand. For the crystallization of the hVDR-1,25(OH)$_2D_3$ complex, a truncated form of the hVDR LBD was used: 50 amino acid residues from a large insertion domain at the N-terminal part of the LBD connecting helices H1 to H3 was deleted. This region is characterized by poor sequence conservation between VDR family members and a predicted disordered state. No clear biological function has been assigned to the insertion region. H12 is in the agonist position, stabilized by two interactions with the ligand, by several hydrophobic contacts with residues of H3, H5 and H11 and two polar interactions with residues of H3 and H4. Some of these residues contact the ligand, thus indicating an additional indirect ligand-control of the position of H12. In the hVDR structure, a strong crystalline contact is observed between helix H3n and helices H3, H4 and H12 of a symmetrically related molecule, with H3n mimicking coactivator peptide contacts.

In this crystal structure, the A-ring of 1,25(OH)$_2D_3$ in its VDR LBP, adopts a chair B conformation with the 19-methylene “up” and the 1α-OH and 3β-OH groups in equatorial and axial orientations, respectively. The aliphatic chain at position 17 of the D-ring adopts an extended conformation (Fig. 5B), different from those observed for the 1,25(OH)$_2D_3$ complexes with CYPs or DBP. The ligand is buried in closed binding pocket and forms extensive interactions. The conformation of the ligand is maintained through the interactions of two types: first, with the hydrophobic residues lining the LBP and, second, through the hydrogen bonds formed between polar residues and three hydroxyl groups of the ligand. The main anchoring interaction points are: the 1α-OH group with Ser237 (H3) and Arg274 (H5), the 3α-OH group with Ser278 (H5) and Tyr143 (loop H1–H2) and the 25-OH group with His305 (loop H6–H7) and His397 (H11) (Fig. 5B). The triene connecting the A-

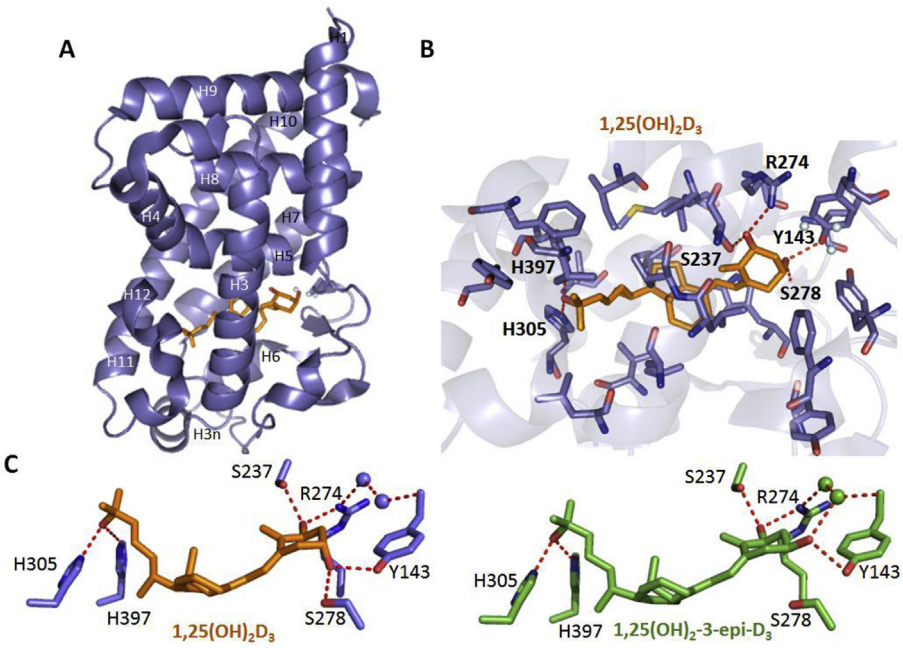

Fig. 5. hVDR-1,25(OH)$_2D_3$ crystal structure. (A) Overall structure of hVDR LBD. The VDR LBD bound to 1,25(OH)$_2D_3$ is composed of 13 helices (H1,2, 2n,3–12). (B) Conformation of 1,25(OH)$_2D_3$ in the LBP. 1,25(OH)$_2D_3$ is shown in stick representation in orange. (B) Binding mode of 1,25(OH)$_2D_3$ (in orange) in the VDR LBP. Specific H-bonds anchoring the three hydroxyl-groups of the 1,25(OH)$_2D_3$ are shown as dash lines. (C) Binding mode of 1,25(OH)$_2D_3$ (in green) and 1,25(OH)$_2$-3-epi-D$_3$ (in blue) in the LBP of hVDR. The hydrogen bonds are in green and blue dashed lines.

Please cite this article in press as: Rochel, N., Molnár, F., Structural aspects of Vitamin D endocrinology, Molecular and Cellular Endocrinology (2017), http://dx.doi.org/10.1016/j.mce.2017.02.046

and C-ring is tightly sandwiched in a hydrophobic channel between Ser275 (loop H5-β) and Trp286 (β1) on one side and Leu233 (H3) on the other side. The C ring contacts Trp286 while the C-18 methyl group points toward Val234 (H3). The side chain is surrounded by hydrophobic residues. The LBP of hVDR is large (697 $Å^3$) with the $1,25(OH)_2D_3$ occupying only 56% of its volume. A channel of water molecules near the position C-2 of the A-ring creates an extra-cavity; additional space around the aliphatic chain is also observed.

4.2. Rat and zebrafish VDR LBD-$1,25(OH)_2D_3$ complexes

VDR LBDs from two other species, *rat norvegicus* (rVDR) (Vanhooke *et al.*, 2004) and *danio rerio* (zVDR) (Ciesielski *et al.*, 2004, 2007) have been also crystallized. In case of rVDR LBD (PDB ID: 1RK3), the same truncation of the large insertion region connecting helices H1 to H3 as for hVDR was applied. For the zVDR LBD (PDB ID: 2HC4), a wild-type (wt) protein was used; however, the insertion region was not visible in the electron density maps indicating its high flexibility resulting in a static disorder. The differences observed between the structures of h, r and z VDR LBDs are small and primarily involve the loops. The LBP is conserved both in sequence and structure, and the ligand conformation, and interactions observed in all crystal structures are very similar.

In contrast to hVDR LBD co-crystallized with ligand in the absence of coactivator peptide, rVDR and the zVDR LBDs were crystallized in presence of additional coactivator peptides that were added in order to stabilize the complexes and promote crystal growth. For the rVDR complexes the second LXXLL motif of DRIP205/Med1 has been used (Vanhooke *et al.*, 2004) and for the zVDR the second LXXLL motif of SRC-1 or SRC-2 (Ciesielski *et al.*, 2004, 2007). The LXXLL peptides observed in the crystal structures of z and rVDR are bound to a groove formed by helices H3, H5 and H12 of the LBD. For the LXXLL motif of DRIP205/Med1 (625–636 KNHPMLMNLLKD) this interaction buries about 507 $Å^2$ of the receptor's surface. The side chains of Leu630, 633, and 634 of a peptide are buried within the pocket and surrounded by hydrophobic residues, while Met631 and Asn632 are oriented outwards from the solvent (Fig. 6). Coactivator peptide is additionally locked through the hydrogen bonds between Glu416 from H12 (hGlu420) with the backbone amide nitrogen of Leu630 and Leu633. At the other end, Lys242 from H3 (hLys246) forms a hydrogen bond to the main chain oxygen of Leu634. The same binding is observed for the zVDR LBD-peptide-ligand complex. The interactions of coactivator peptides to VDR are similar to those described for other NRs (Darimont *et al.*, 1998; Nolte *et al.*, 1998; Shiau *et al.*, 1998).

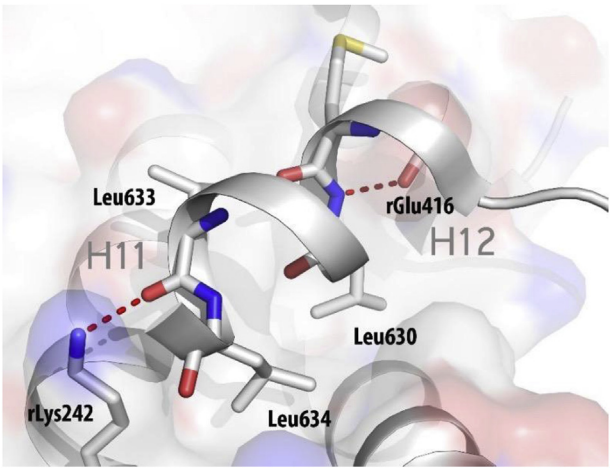

Fig. 6. Binding mode of the DRIP205/Med1 coactivator peptide LXXLL to rVDR LBD.

4.3. Structural insight into VDR LBD binding by natural metabolites

As mentioned previously, $1,25(OH)_2D_3$ is subjected to enzymatic inactivation via two major pathways leading to C-24 and C-23 hydroxylated metabolites in various tissues. The 24-hydroxylation, is generally considered as the first step in the degradation pathway of $1,25(OH)_2D_3$ (Prosser and Jones, 2004). However, some data have demonstrated that both $1,25(OH)_2D_3$ and the 24-hydroxylated metabolite $1\alpha,24R,25\text{-}(OH)_3D_3$ induced gene transcription (van Driel *et al.*, 2006). Thus, not only $1,25(OH)_2D_3$, but also the presumed 24-hydroxylated "degradation" products stimulate differentiation of human osteoblasts through VDR activation. In addition, other natural metabolite, $1\beta,25(OH)_2D_3$, acts in bone as an agonist and directly stimulates mineralization in a nuclear VDR-dependent way (Norman *et al.*, 1993).

Another metabolite modified at the A-ring, the $1,25(OH)_2$-3-epi-D_3, initially identified in the culture of human neonatal keratinocytes, has been shown to retain significant biological activity compared to the natural hormone (Molnár *et al.*, 2011; Reddy *et al.*, 2000). The crystal structural analysis of the VDR-$1,25(OH)_2$-3-epi-D_3 (PDB ID: 3A78) showed that VDR displays specific adaptation of the LBP (Fig. 5C) (Molnár *et al.*, 2011). Although the two diastereomers differ only in the position of the C3–OH group, the $1,25(OH)_2$-3-epi-D_3 takes a slightly more compact conformation in the LBP. While the 1α-OH and 25α-OH display the canonical hydrogen bonds, the 3-epi-OH of $1,25(OH)_2$-3epi-D_3 interacts through hydrogen bonding only with Tyr143 instead of interacting with both Tyr143 and Ser278. A significant feature of the $1,25(OH)_2$-3-epi-D_3 is the compensation of the loss of interaction with Ser278 by a water-mediated hydrogen bond.

4.4. Dynamic process of ligand binding

X-ray crystallography has provided detailed information on the molecular mechanism of VDR LBD action. However, the crystal structures give only a static view of the ligand binding process. The dynamics of ligand binding process by VDR has been investigated using complementary methods to X-ray crystallography such as NMR (Singarapu *et al.*, 2011) and Hydrogen/Deuterium exchange (HDX) coupled with mass spectrometry (MS) (Zhang *et al.*, 2010). HDX-MS analysis has been used to probe the conformational dynamics upon ligand binding to VDR. Within the apo form VDR LBD, the entire C-terminal part has been shown to be very dynamic with 80% of amide hydrogen exchange (Zhang *et al.*, 2010). The region forming the LBP also showed high exchange rate, while the central layer of the α-helical sandwich and H10 appeared protected. As expected, binding of $1,25(OH)_2D_3$ led to significant protection from hydrogen amide exchange. Interestingly, regions remote from the LBP, such as loop 7–8 and helix H10, displayed altered HDX profile upon ligand binding. H10 forms an interface for heterodimerization with RXR; therefore, the destabilization of this region in the holo-form of VDR is intriguing. Impaired protection from the amide hydrogen exchange was observed for the VDR complex with alfacalcidol, a precursor of $1,25(OH)_2D_3$ lacking a 25-OH group. Formation of a less stable complex explains partial agonistic behavior of alfacalcidol. Singarapu *et al.* reported assigned NMR chemical shifts of rVDR-LBD in presence of $1,25(OH)_2D_3$ or synthetic ligands (Singarapu *et al.*, 2011). The comparison of apo- and holo-forms of VDR LBD revealed significant conformational changes upon the ligand binding.

5. Mutations of VDR found in HVDRR

The presence of the VDR with altered function is characteristic of hereditary vitamin D-resistant rickets type 2 (HVDRR) that

shows a phenotype connected with softening and weakening of the bones associated with alopecia in some cases. The alterations in the VDR gene are caused by mutations that prevent VDR protein from functioning properly. The mutations may create abnormally short VDR with premature termination of the translation (STOP codons) or result in VDR with altering some of its function as molecular machine affecting ligand- or DNA-binding, heterodimerization with RXR or coregulator-binding. The overall effect of the mutation may also be the combinatorial result that affects all four functions at the same time. This leads to suboptimal gene regulatory responses even though the presence of $1,25(OH)_2D_3$ in the body. Mutations are found in either the DBD or in the LBD. Figs. 7 and 9 show the schematic (A) and structural (B) location of known mutations in the DBD and LBD identified in HVDRR patients. We will now discussed the structural implications of these mutations based on structural data or modeling. Two structural studies have investigated the structural features of HVDRR mutations, His305Gln (Rochel *et al.*, 2010) and Arg270Leu/Trp282Arg (Nakabayashi *et al.*, 2013).

5.1. Structural implications of HVDRR-associated VDR DBD mutants

In the VDR DBD, 11 missense mutations (Fig. 7) have been identified in patients all affected by alopecia (Feldman and Malloy, 2014). Most of them (8 from 11) introduce a reversed/neutral residues in the place of a positively charged amino acids (histidine or arginine) such as His35Gln, Lys45Glu, Arg50Gln, Arg73Gln and Arg80Gln thus directly disrupting the DNA (−) and protein (+) interaction.

Among those residues, His35 forms a stabilizing hydrogen bond with Thr32 (Fig. 8C) and the introduction of glutamine (His35Gln) creates a clash with Thr40, Phe36 or Lys45 in addition to the loss of the hydrogen bond, leading to destabilization of DNA binding. The other charged residues that were found mutated (Lys45, Arg50, Arg73 and Arg80) directly interact with DNA (Fig. 8A–C). Mutation of Lys45 to a negatively charged glutamate creates a repulsion with dA402 phosphate group, while for Arg50Gln, Arg73Gln and Arg80Gln, the glutamate either abolishes the interaction dT430 nucleotide due to neutral change or weakens the interaction with dG431 nucleotide.

Some other mutations found in the DBD are targeting small residues that are mutated into bulkier or even larger negatively charged ones creating perturbations that directly interfere with the DNA-binding such as Val26Met, Gly33Asp and Gly46Asp. The Val26Met mutation introduces a larger methionine that is expected to clash with the surrounding residues and thus destabilizing the first zinc finger. In case of Gly33Asp mutation the larger negatively charged residue also clashes with the surrounding residues destabilizing dT402 nucleotide and the β-sheet region e.g. His35. For Gly46Asp mutant, the negatively charged aspartate residue is expected to prevent the interactions of Lys45 and Arg50 with DNA.

The remaining mutations in VDR DBD destabilize the fold of the VDR DBD: i) For Cys41Tyr that coordinates the zinc atom in the first zinc finger, the tyrosine clashes with the surrounding residues of the first zinc finger and destabilize it; ii) Phe47Ile mutation disrupts the stacking π-π interactions with Phe58 (Fig. 8B) and iii) In Cys84Arg, the larger positively charged arginine clashes with Phe47, Phe48, Leu81 and Met89 and destabilizing α2 recognition helix.

5.2. Structural implications of HVDRR-associated VDR LBD mutants

In the LBD of VDR around 20 mutations (Fig. 9) have been identified in HVDRR patients. Mutations at Arg274 and His305 affect directly the hydrogen bond anchoring points of the ligand (Fig. 9A, residues in red), while Leu227, Ile268, Trp286 and Ile314 mutations affect hydrophobic contacts (Fig. 9A, residues in green) for $1,25(OH)_2D_3$ binding, whereas Gln259, Glu329 and Arg391 (Fig. 9A, residues in orange) have effect on heterodimerization with RXR. Residue Glu420 (Fig. 9A, in blue) anchors the cofactor as shown previously (Fig. 6). The structural implications for these and some other missense mutations in VDR LBD will be now discussed.

5.2.1. Thr146Ile VDR mutant

Thr146 is located in the loop between helices H1 and H2 (Fig. 9), a region with a possible entry point for VDR ligands. Taking its

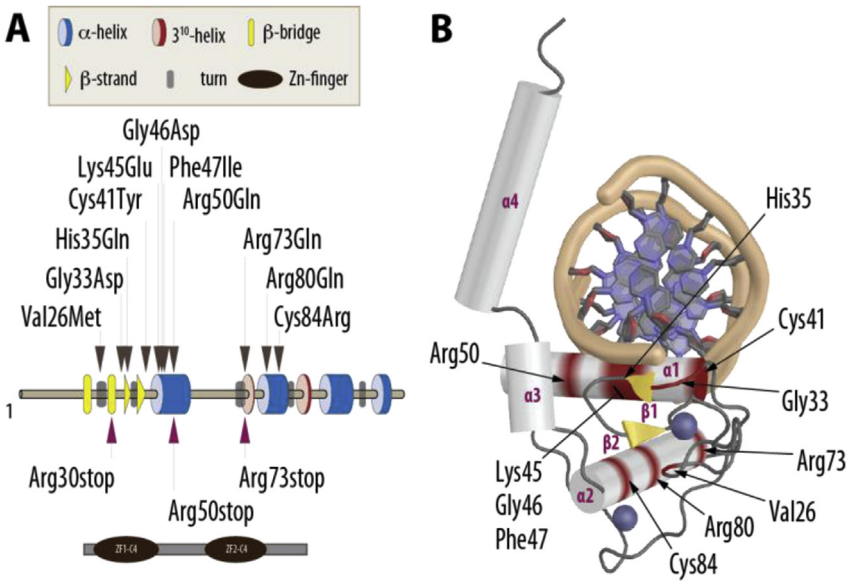

Fig. 7. The location of HVDRR mutations in the hVDR DBD. (A) Schematic and (B) structural location of the identified mutations is shown. The structural information is based on PDB ID: 1YNW. Helices are numbered α1-4 and the beta sheets β1-2. The α4 is part of the hinge region.

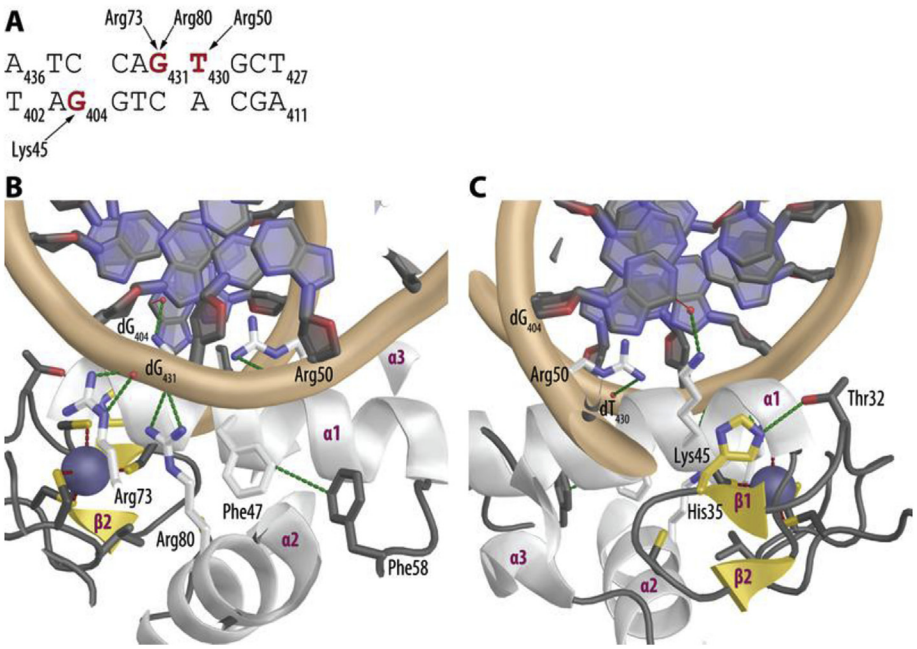

Fig. 8. The specific interaction of VDR DBD and DNA. Some of the affected DNA-interacting residues as well as those involved in intramolecular stabilization are highlighted.

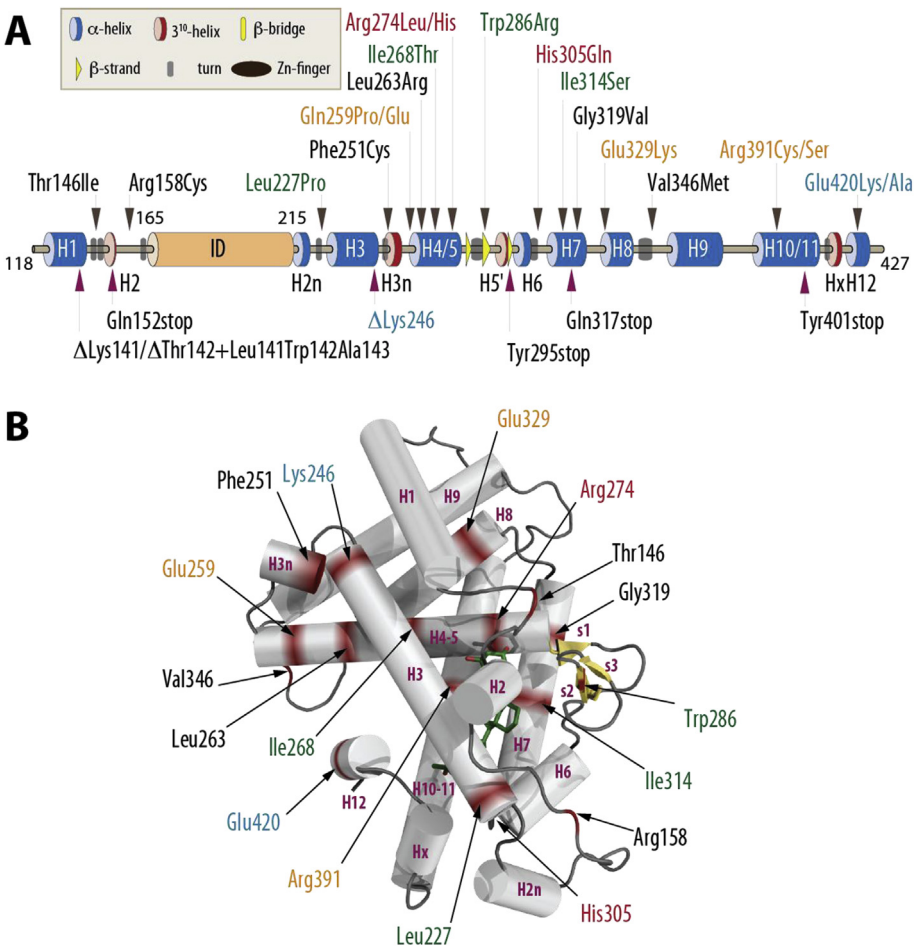

Fig. 9. The location of HVDRR mutations in the hVDR LBD. (A) Schematic and (B) structural location of the identified mutations is shown. The structural information is based on PDB ID: 1DB1. Residues that directly contribute to $1,25(OH)_2D_3$ binding are highlighted in red (H-bond anchoring points) and green (hydrophobic contacts) color. Residues know to affect heterodimerization with RXR are in orange and amino acids that are part of the coactivator-binding charge-clamp are in blue.

Please cite this article in press as: Rochel, N., Molnár, F., Structural aspects of Vitamin D endocrinology, Molecular and Cellular Endocrinology (2017), http://dx.doi.org/10.1016/j.mce.2017.02.046

hydrophilic nature, it is located on the surface and faces outside. The structural impact is difficult to evaluate as Thr146Ile mutant has no direct involvement in the $1,25(OH)_2D_3$ binding or heterodimerization and effect on cofactor binding is not available. This mutation together with a second mutation, Arg158Cys, is found in a Korean patient without alopecia (Malloy and Feldman, 2011).

5.2.2. Arg158Cys VDR mutant

Arg158Cys mutated VDR showed a 3× lower *in vitro* transactivation potential in COS-7 cells and lack of *CYP24A1* gene expression in isolated patient fibroblasts. Arg158 is located in one of the two nuclear localization signals in the VDR (Hsieh *et al.*, 1998) thus a reduction in VDR's nuclear transport may be expected. From a structural point of view, Arg158 is part of a complex hydrogen bond network involving Asp292 (H6), Asp299 and Lys294 (both from β-sheet region) as well as water-mediated contacts with other residues and the backbone of the β-sheet region. Thus the Arg158Cys destabilizes this region most notably Trp286 position that translates into decreased $1,25(OH)_2D_3$ binding and direct effect on target gene activation.

5.2.3. Leu227Pro VDR mutant

Leu227, located at the N-terminal part of helix H3 (Fig. 9), creates a hydrophobic interaction with one of the methyl groups of the aliphatic $1,25(OH)_2D_3$ chain and participates in helix H11 stabilization. The Leu227Pro mutation, by introducing a rigid proline backbone into an α-helix, breaks this secondary structure affecting all the neighbor interactions including direct interaction with $1,25(OH)_2D_3$. The phenotype of this mutation is associated with absence of alopecia (Huang *et al.*, 2013).

5.2.4. Lys246 VDR mutant

Lys246, located in helix H3 (Fig. 9), directly interacts with the coactivator and through water mediated contact with Gln259 (see below Gln259). Lys246 together with Glu420 forms a charge clamp for the interaction of the LXXLL motif of the coactivators. The ΔLys246 mutation shortens H3, creates spatial irregularities in the topology of H3 and 4 and removes an important coactivator contact point. Through allostery, it may affect also the heterodimerization with RXR. However, it does not affect directly the ligand-binding and corepressor interaction with Hairless (Zhou *et al.*, 2009).

5.2.5. Phe251Cys VDR mutant

Phe251 acts as a space-filler between helices H3 and H4 (Fig. 9) creating a small ordered helical structure e.g. H3n. It has been suggested that the mutation Phe251Cys directly interferes with RXR heterodimerization (Malloy *et al.*, 2001), though this effect will be based on allostery. Although the location of Phe251 is very close to the cofactor binding site with Leu694 distanced at 3.9 Å, it most likely destabilizes the middle layer of the LBD sandwich through increasing helix H4 fluctuation. Ectopic RXR in *in vitro* transactivation assay and increased $1,25(OH)_2D_3$ rescues VDR's activity to some extend (Malloy *et al.*, 2001), through allosteric effects via RXR heterodimerization as well as further stabilization upon $1,25(OH)_2D_3$ binding with subsequent increase in coactivator binding.

5.2.6. Gln259Pro VDR mutant

Gln259 located in helix H4 (Fig. 9), similarly to Phe251, stabilizes both helices H3 and H4. It interacts directly with Leu254 (loop between H3 and H4) and through water molecule with Lys246 holding it in position for effective coactivator interaction. The mutation Gln259Pro has been proposed to directly affect the RXR heterodimerization (Cockerill *et al.*, 1997) though it is rather improbable since its position is far from the heterodimerization interface. However, its interaction with Lys246 directly affects the coactivator binding and allosterically may impact the dimerization. The phenotype of this mutation is associated with alopecia (Cockerill *et al.*, 1997). Gln259Glu has been also identified in Brazilian patients, where the DNA- and ligand-binding of VDR is not affected so dramatically nor the *in vitro* transactivation potential of the *CYP24A1* promoter (Macedo *et al.*, 2008).

5.2.7. Leu263Arg VDR mutant

Leu263, located in helix H4 (Fig. 9), points to the void area towards coactivator binding site and despite being far from directly interacting with it, it clearly contributes to the hydrophobicity of this region. The larger positively charged arginine residue in Leu263Arg disrupts this property and the longer arginine side chain may clash with the neighboring residues. It also creates spatial distortions affecting the coactivator binding and allosterically the other parts of the LBD. This is supported by experimental GST-pull down that shows for Leu263Arg 25% of SRC1 interaction and 30% of $1,25(OH)_2D_3$ binding compared to wt VDR (Nguyen *et al.*, 2006).

5.2.8. Ile268Thr VDR mutant

The Ile268Thr mutation has been identified in a young Saudi Arabian girl without alopecia (Malloy *et al.*, 2004). Ile268Thr shows 5- to 10-fold lower affinity for $1,25(OH)_2D_3$, but can be stabilized and rescued by 20-epi-$1,25(OH)_2D_3$. This mutation weakens slightly the RXR or coactivator interactions and it has been suggested that its effect comes from a direct contact with $1,25(OH)_2D_3$. Located in helix H5, Ile268 is in the close proximity of $1,25(OH)_2D_3$ (C22 at closest 4.3 Å) and 4.1 Å from Phe422 (H12), critical for coactivator binding. The smaller hydrophilic threonine locally disrupts the hydrophobicity of the LBP and its interaction with the ligand by creating a spatial void. In addition, some rotamers of Thr268 may clash with Phe422 thus destabilizing the position of helix H12. The rescue of the activity by 20-epi-$1,25(OH)_2D_3$ is the consequence of the different conformation of the side chain of this analog that is located closer to Thr268 thus filling the created void.

5.2.9. Arg274Leu VDR mutant

Arg274Leu mutation has >1000-fold reduction of $1,25(OH)_2D_3$ responsiveness (Kristjansson *et al.*, 1993). This mutant VDR, rArg270Leu (hArg274Leu), is one of the mutations structurally investigated. The overall fold and active protein topology is maintained (Nakabayashi *et al.*, 2013). Small disturbances are observed near the mutation site such as Cα shifts creating additional space (Fig. 10B, red circle) or the appearance of the two placeholder water molecules (red arrows). One of them contacts the 1α-OH (Fig. 10B) and the second is linked to Thr142 main chain carbonyl group. However, these interactions are weaker than the direct interaction of the ligand with e.g. 1α-OH in the wild type protein (Fig. 10A), thus leading to lower binding affinity for $1,25(OH)_2D_3$.

In addition to Arg274Leu, Arg274His mutation has also been identified (Allubeh *et al.*, 2011). The histidine residue compared to arginine has a shorter, inflexible side chain that would take a suboptimal distance from 1α-OH of the $1,25(OH)_2D_3$ and the bulkier imidazole moiety may clash with the neighboring residues disrupting the interaction with Thr142 in the C-terminal part of the H1.

5.2.10. Trp286Arg VDR mutant

Trp286 is involved in numerous intramolecular interactions with other residues that stabilize the molecular structure of VDR. In addition, it serves as a stabilizing π-π bond "bottom tray" for the CD rings of $1,25(OH)_2D_3$ and is essential for its activity. The Trp286Arg mutation has been identified in patients exhibiting severe rickets without alopecia (Nguyen et al., 2002). In the crystal structure of

Please cite this article in press as: Rochel, N., Molnár, F., Structural aspects of Vitamin D endocrinology, Molecular and Cellular Endocrinology (2017), http://dx.doi.org/10.1016/j.mce.2017.02.046

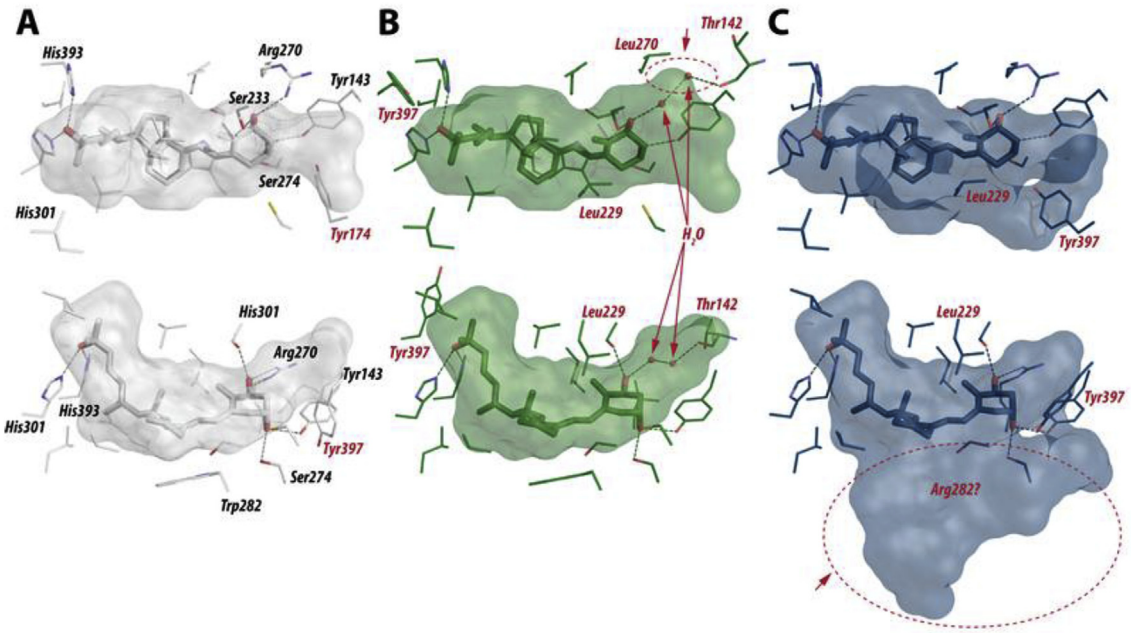

Fig. 10. Structural mechanism of rArg270Leu and rTrp282Arg HVDRR mutant in the presence $1,25(OH)_2D_3$. (White = wt, green = Arg270Leu-VDR and blue = Trp282Arg-VDR).

rVDR(Trp282Arg(hTrp286Arg))-$1,25(OH)_2D_3$ complex (Nakabayashi *et al.*, 2013), the Arg282 neighbor residues (Asp278-Gln287) are not visible because of their high fluctuation, probably leading to local destabilization of the β-strand and the beginning of loop H1−H2 though the overall VDR structural fold is still maintained (Fig. 10C). However, in this structure all the anchoring OH interactions are strictly maintained and $1,25(OH)_2D_3$ is bound (Fig. 10C). Experimental circular dichroism data from solution based measurement show partial or no binding at all for Trp282Arg, compared to the wt receptor. Structural artefacts may be present by altering the equilibrium towards active/ligand bound protein with the presence of a high ratio of coactivator peptides in the crystallization process.

5.2.11. His305Gln VDR mutant

His305Gln VDR mutant shows 10% transactivation potential and 8-fold lower affinity for $1,25(OH)_2D_3$ compared to wt VDR (Malloy *et al.*, 1997). The crystal structure of hVDR(His305Gln)-$1,25(OH)_2D_3$ complex maintains the main topological features such as overall fold and agonistic conformation (Rochel *et al.*, 2010). The expected difference around Gln305 residue is manifested by “broad cloud of electron density”, which highlights the possibility of an existence of two distinct conformers. In the wt VDR the interaction with His305 (hydrogen bond acceptor) and His397 (hydrogen bond donor) is essential for the efficient recognition of $1,25(OH)_2D_3$ as well as other analogues. However, the weaker His305Gln-$1,25(OH)_2D_3$ (Fig. 11A top) bonding creates a distortion in H6 and 7 through conformational changes of Val300 and Glu311 positions, respectively (Fig. 11A bottom). This leads to the loss of two hydrogen bonds between Ser306 and Gln400 and Gln400 and His305 (Fig. 11B top and bottom). As a consequence, the loosen Gln305 adopts two different side chain conformations. Overall these stabilizing interactions are reflected in lower efficacy of $1,25(OH)_2D_3$ in His305Gln VDR transcriptional activity.

5.2.12. Ile314Ser VDR mutant

Ile314, from helix H7 (Fig. 9), is part of a hydrophobic network around H6 and H7, opposite to H12 and has been known to be important for the binding of some VDR analogs such as MC1288 or Gemini by modulating the position of the side chains in this region (Molnár *et al.*, 2006). The transactivation ability of Ile314Ser is reduced, but can be restored by excess of $1,25(OH)_2D_3$ and it nearly completely cures these patients. Additional experiments using patient fibroblasts/transfected cells also indicate that the addition of RXR somewhat augments the activity of Ile314Ser (Whitfield *et al.*, 1996).

5.2.13. Gly319Val VDR mutant

Gly319, also located in helix H7 (Fig. 9), is in the vicinity of the C-terminal end of helix H3 partly facing outside towards the LBD surface. There is a possibility that a hydrophobic residue at this position, exposed to the solvated hydrophilic surrounding, will deform H7. This may affect the intramolecular stability of this region, but not so critically as other mutations. Indeed, a patient bearing the Gly319Val mutation had a normal bone mass acquisition during young adulthood, but displayed full alopecia. It is intriguing to see the uncoupling of these two processes although normally both would require fully functional VDR (Damiani *et al.*, 2015). However, the detailed functional data is not available for this mutation.

5.2.14. Glu329Lys VDR mutant

Glu329 from helix H8 is in the vicinity of the C-terminal part of H9 and the N-terminal part of H10 (Fig. 9). It is surrounded, but does not directly interact with His326 (H9), His371 (H10) and Tyr366 (H10) and stabilizes this region. It has been proposed to be important for heterodimerization (Malloy and Feldman, 2010), though no direct contribution can be expected. The introduction of the longer arginine with positive charge leads to destabilization of this region by disrupting charged residue pair attractions and possibly also clashing with His326, His371, Tyr366, Leu379 and Gly375. It is however difficult to judge *in vivo* the contribution of Glu329Lys alone because in the same patient an additional frameshift in exon 4 (both heterozygous mutations) leading to truncated VDR has been also detected (Miller *et al.*, 2001).

Please cite this article in press as: Rochel, N., Molnár, F., Structural aspects of Vitamin D endocrinology, Molecular and Cellular Endocrinology (2017), http://dx.doi.org/10.1016/j.mce.2017.02.046

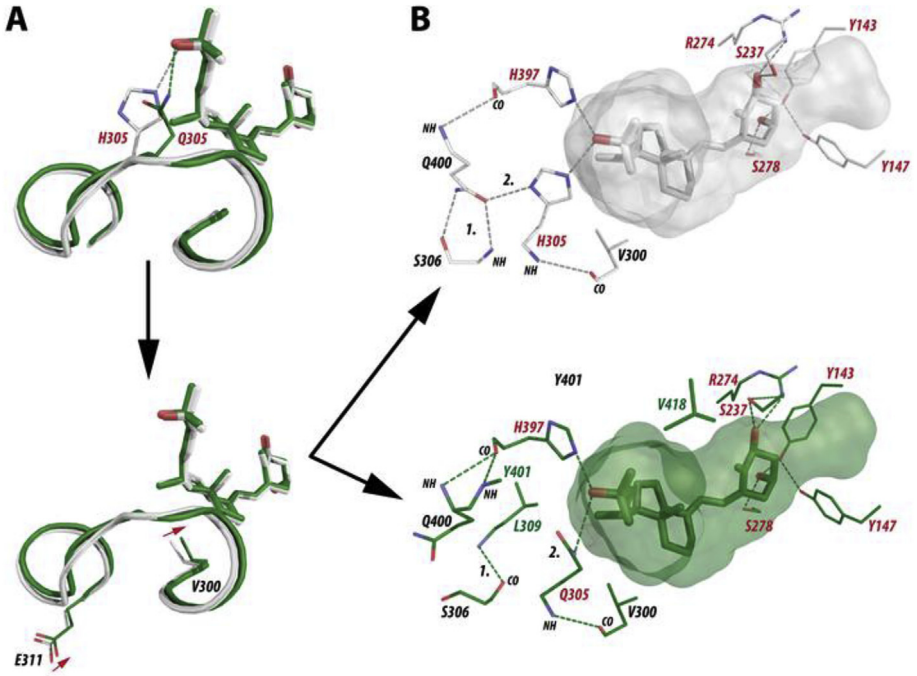

Fig. 11. Structural mechanism of His305Gln HVDRR mutant. (White = wt and green = His305Gln-VDR).

5.2.15. Val346Met VDR mutant

Val346 in the loop between helices H8 and H9 (Fig. 9) is surrounded by hydrophobic residues at distance larger than 4 Å. Without doubt it contributes to the hydrophobic character of this region. Val346Met mutation was identified in a patient displaying alopecia, papular lesions on the scalp and face (Arita *et al.*, 2008). In addition to this phenotype the patients had mild hearing loss and secondary speech abnormalities. Although it has not been reported before in humans, the VDR knockout mice has progressive hearing loss (Zou *et al.*, 2008). From the structural point of view the introduction of less hydrophobic but longer methionine, which clashes with all the residues around, destabilizes the whole region and with high possibility repositions Arg391, which directly interacts with RXR (see below).

5.2.16. Arg391 VDR mutants

Arg391 from helix H10 (Fig. 9) has a very unique role in the interaction with RXR as well as stabilization of VDR itself. It interacts with Ser340 and Asp342, positions Asp342 towards Arg348 (RXR) and Ser427 (RXR). Thus both Arg391Cys and Arg391Ser mutants, by introducing smaller residues, dramatically disrupt the RXR heterodimerization interface and also destabilize helices H10-11 and loop 8–9 without direct effect on ligand binding though an allosteric effect cannot be excluded. The transcriptional activity of Arg391Cys cannot be restored with pharmacological doses of a vitamin D derivative and the best improvement has been experimentally achieved with the excess of both of RXR and $1,25(OH)_2D_3$ (Whitfield *et al.*, 1996). In addition to the cysteine mutation a serine mutation has been identified though the exact contribution of Arg391Ser *in vivo* is difficult to attribute as the mutation is present together with Leu263Arg mutation (Nguyen *et al.*, 2006). The serine residue, though capable of creating hydrogen bonds, is much shorter than arginine thus unable to maintain the original interaction network.

5.2.17. Glu420 VDR mutants

Glu420 is one of the critical residues due to its location in the activation helix H12 (Fig. 9) and its involvement in numerous interactions and intramolecular stabilization within the LBD. Firstly, its interaction with Lys264 in helix H4 provides a mutual stabilization. Secondly, the subsequent optimal positioning of the charge clamp for both Lys246 and Glu420 residues facilitates coactivator binding. Its mutation to smaller Ala (Glu420Ala) or positively charged Lys (Glu420Lys) disables any of the above described processes. Interestingly, the Glu420Lys mutation has no defect on ligand binding, RXR heterodimerization or DNA-binding (Malloy *et al.*, 2002). Very surprisingly this mutation although having all the phenotypes of full-blown rickets it does not manifest alopecia.

6. Allosteric effect of $1,25(OH)_2D_3$ within intact VDR-RXR complex

The structure of the full length VDR-RXR complex has been investigated in solution by two different structural methods, by small angle X-ray scattering (SAXS) (Rochel *et al.*, 2011) and cryo-electron microscopy (cryo-EM) (Orlov *et al.*, 2012). These studies have yielded further new knowledge about the quaternary structure of the intact VDR-RXR complex with DNA and the allosteric interplay between the different binding domains. Comparison of the LBD and DBD domains of this multidomain structure with those of previously solved individual domain structures showed structural conservation. The solution structures show that DBDs and LBDs are separated and positioned asymmetrically (Fig. 12). The relative position of the domains and the observed asymmetry of the overall architecture both point to the essential role played by the hinge domains in establishing and maintaining the integrity of the functional structures. While the RXR hinge has a not well-defined structure, the hinge domain of VDR forms an α-helix that stabilizes the whole complex, thus facilitating the positioning of the LBD and the surface to be accessible by the coregulators.

Please cite this article in press as: Rochel, N., Molnár, F., Structural aspects of Vitamin D endocrinology, Molecular and Cellular Endocrinology (2017), http://dx.doi.org/10.1016/j.mce.2017.02.046

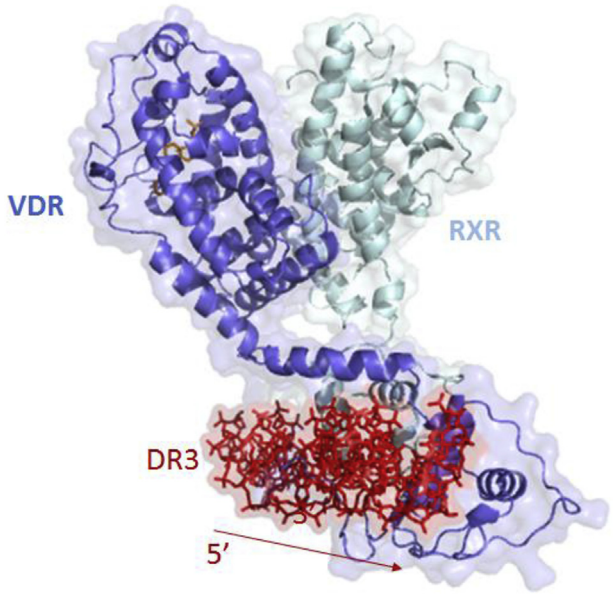

Fig. 12. 3D structure of VDR–RXR heterodimer bound to DNA DR3 response element obtained by solution studies.

The mechanisms of allostery in these receptors focuse on the coupling between the LBD, the cofactor binding regions, and the DBD. It has been shown that the dynamics of LBDs is affected by the interaction with DNA and that ligand-induced activation is dependent on the anchoring DNA sequence (Zhang *et al.*, 2011). Although significant structural differences between isolated, complexed domains and DNA bound dimers have not been detected, there is an evidence of long-range allosteric communication between the domains as revealed by Hydrogen Deuterium Exchange (HDX)-Mass Spectrometry (Zhang *et al.*, 2011). These studies indicated cooperative effects between the VDR DBD and LBD to fine tune transcriptional regulation by the ligands and the DNA. Upon $1,25(OH)_2D_3$ binding to full length VDR-RXR, the HDX profile was very similar to the binding to VDR LBD alone with a stabilization of VDR H12. Interestingly, an increase of solvent exchange in the DBD of VDR was also observed upon ligand binding, indicating that the ligand has an impact on the DBD conformation. Upon ligand binding, a stabilization of the heterodimer interface was also observed. The HDX profile of $1,25(OH)_2D_3$ binding in the presence of RXR ligand, was similar to that of $1,25(OH)_2D_3$ alone. Moreover, the binding of VDR-RXR heterodimers to various DNA sequence alters the receptor dynamics in regions not in contact with the DBDs, such as the coactivator binding surfaces.

Coregulator recruitment by NR complexes exert additional allosteric control over the resulting structure and receptor function. Hundreds of transcriptional coregulator proteins are recognized by NRs, and there are likely multiple mechanisms of interaction of these proteins with NRs. The only available structural data at atomic resolution on NR-coregulators interactions concerned short peptide of the coregulators, containing the LXXLL motif that recognizes a specific groove on the surface of the NR LBD as mentioned previously. However, the binding of coregulators in the LBD of NRs can be associated with different degrees of asymmetry in the relative ability of each LBD to bind a cofactor, even for homodimeric NRs as shown on RAR homodimer (Osz *et al.*, 2012). This asymmetry is even larger for full coregulator proteins.

7. Conclusion and perspectives

In human, the synthesis and metabolism of natural vitamin D derivatives is under strict control of different enzymes located in various tissues. In addition, their transport and elimination as well as action on transcriptional regulation involves the harmonic cooperation of diverse proteins with vitamin D binding capacities such as DBP or VDR. VDR and its ligands, besides their classical role in the regulation of calcium and phosphate homeostasis engage in large variety of processes spanning from cell cycle regulation (proliferation/differentiation/apoptosis), modulation of the adaptive/innate immune system to direct alterations of metabolic pathways.

While the X-ray crystallography provided the atomic details of protein–ligand interactions and ligand specificity by the different proteins involved in vitamin D endocrinology, other techniques such as HDX-MS and NMR have provided information about the conformational dynamics of protein upon ligand binding in solution and solution structural methods insights into full VDR-RXR complexes structure and function. The ligand-, DNA-, or coactivator-binding and heterodimerization with RXR cannot be uncoupled because of the extensive allosteric communication inside of the VDR-RXR heterodimer. The net effect on the level and target specific regulation will be achieved by the contribution from all this processes. Remaining questions concern the role of RXR and its ligands in VDR mediated gene regulation and the structural and functional characterization of the VDR-RXR associated complexes that represent an excellent challenge for the future for a deeper understanding of the mechanism of action of vitamin D endocrinology.

Acknowledgement

This work was supported by IGBMC institute funds from CNRS, Inserm and Université de Strasbourg and Grants from the Agence Nationale de Recherche (ANR-13-BSV8-0024-01), the Fondation ARC pour la Recherche sur le Cancer, La Ligue Contre le Cancer, L'Alsace Contre le Cancer and the Fondation pour la Recherche Médicale (FRM).

References

Aljubeh, J.M., Wang, J., Al-Remeithi, S.S., Malloy, P.J., Feldman, D., 2011. Report of two unrelated patients with hereditary vitamin D resistant rickets due to the same novel mutation in the vitamin D receptor. J. Pediatr. Endocrinol. Metab. 24, 793–799.

Annalora, A.J., Goodin, D.B., Hong, W.X., Zhang, Q., Johnson, E.F., Stout, C.D., 2010. Crystal structure of CYP24A1, a mitochondrial cytochrome P450 involved in vitamin D metabolism. J. Mol. Biol. 19, 441–451.

Arita, K., Nanda, A., Wessagowit, V., Akiyama, M., Alsaleh, Q.A., McGrath, J.A., 2008. A novel mutation in the VDR gene in hereditary vitamin D-resistant rickets. Br. J. Dermatol 158, 168–171.

Belorusova, A.Y., Rochel, N., 2014. Modulators of vitamin D nuclear receptor: recent advances from structural studies. Curr. Top. Med. Chem. 14, 2368–2377.

Bikle, D.D., Chang, S., Crumrine, D., Elalieh, H., Man, M.Q., Choi, E.H., Dardenne, O., Xie, Z., Arnaud, R.S., Feingold, K., Elias, P.M., 2004. 25-Hydroxyvitamin D 1 α -hydroxylase is required for optimal epidermal differentiation and permeability barrier homeostasis. J. Invest. Dermatol 122, 984–992.

Bouillon, R., Eelen, G., Verlinden, L., Mathieu, C., Carmeliet, G., Verstuyf, A., 2006. Vitamin D and cancer. J. Steroid Biochem. Mol. Biol. 102, 156–162.

Carlberg, C., 2014. Genome-wide (over)view on the actions of vitamin D. Front. Physiol. 5, 167.

Ciesielski, F., Rochel, N., Mitschler, A., Kouzmenko, A., Moras, D., 2004. Structural investigation of the ligand binding domain of the zebrafish VDR in complexes with $1\alpha,25(OH)_2D_3$ and Gemini: purification, crystallization and preliminary X-ray diffraction analysis. J. Steroid Biochem. Mol. Biol. 89–90, 55–59.

Ciesielski, F., Rochel, N., Moras, D., 2007. Adaptability of the Vitamin D nuclear receptor to the synthetic ligand Gemini: remodelling the LBP with one side chain rotation. J. Steroid Biochem. Mol. Biol. 103, 235–242.

Cockerill, F.J., Hawa, N.S., Yousaf, N., Hewison, M., O'Riordan, J.L., Farrow, S.M., 1997. Mutations in the vitamin D receptor gene in three kindreds associated with hereditary vitamin D resistant rickets. J. Clin. Endocrinol. Metab. 82, 3156–3160.

Daiger, S.P., Schanfield, M.S., Cavalli-Sforza, L.L., 1975. Group-specific component (Gc) proteins bind vitamin D and 25-hydroxyvitamin D. Proc. Natl. Acad. Sci. U. S. A. 72, 2076–2080.

Damiani, F.M., Martin, R.M., Latronico, A.C., Ferraz-de-Souza, B., 2015. Normal bone mass and normocalcemia in adulthood despite homozygous vitamin D receptor mutations. Osteoporos. Int. 26, 1819–1823.

Darimont, B.D., Wagner, R.L., Apriletti, J.W., Stallcup, M.R., Kushner, P.J., Baxter, J.D., Fletterick, R.J., Yamamoto, K.R., 1998. Structure and specificity of nuclear receptor-coactivator interactions. Gene Dev. 12, 3343–3356.

Feldman, D., Krishnan, V.A., Swami, S., Giovannucci, E., Feldman, J.B., 2014. The role of vitamin D in reducing cancer risk and progression. Nat. Rev. Cancer 14, 342–357.

Feldman, D., Malloy, P.J., 2014. Mutations in the vitamin D receptor and hereditary vitamin D-resistant rickets. Bonekey Rep. 3, 510.

Fraser, D.R., Kodicek, E., 1970. Unique biosynthesis by kidney of a biologically active vitamin D metabolite. Nature 228, 764–766.

Gray, R.W., Omdahl, J.L., Ghazarian, J.G., DeLuca, H.F., 1972. 25-Hydroxycholecalciferol-1-hydroxylase. Subcellular location and properties. J. Biol. Chem. 247, 7528–7532.

Haussler, M.R., Whitfield, G.K., Kaneko, I., Haussler, C.A., Hsieh, D., Hsieh, J.C., Jurutka, P.W., 2013. Molecular mechanisms of vitamin D action. Calcif. Tissue Int. 92, 77–98.

Head, J.F., Swamy, N., Ray, R., 2002. Crystal structure of the complex between actin and human vitamin D-binding protein at 2.5 A resolution. Biochemistry 41, 9015–9020.

Hewison, M., Adams, J.S., 2011. Extrarenal 1α-hydroxylase. In: Feldman, D., Pike, J.W., Adams, J.S. (Eds.), Vitamin D, third ed. Academic Press, San Diego, CA, pp. 777–806.

Hsieh, J.C., Shimizu, Y., Minoshima, S., Shimizu, N., Haussler, C.A., Jurutka, P.W., Haussler, M.R., 1998. Novel nuclear localization signal between the two DNA-binding zinc fingers in the human vitamin D receptor. J. Cell. Biochem. 70, 94–109.

Huang, K., Malloy, P., Feldman, D., Pitukcheewanont, P., 2013. Enteral calcium infusion used successfully as treatment for a patient with hereditary vitamin D resistant rickets (HVDRR) without alopecia: a novel mutation. Gene 512, 554–559.

Kristjansson, K., Rut, A.R., Hewison, M., O'Riordan, J.L., Hughes, M.R., 1993. Two mutations in the hormone binding domain of the vitamin D receptor cause tissue resistance to 1,25 dihydroxyvitamin D_3. J. Clin. Invest. 92, 12–16.

Lin, Z., Li, W., 2016. The roles of vitamin D and its analogs in inflammatory diseases. Curr. Top. Med. Chem. 16, 1242–1261.

Liu, P.T., Stenger, S., Li, H., Wenzel, L., Tan, B.H., Krutzik, S.R., Ochoa, M.T., Schauber, J., Wu, K., Meinken, C., Kamen, D.L., Wagner, M., Bals, R., Steinmeyer, A., Zügel, U., Gallo, R.L., Eisenberg, D., Hewison, M., Hollis, B.W., Adams, J.S., Bloom, B.R., Modlin, R.L., 2006. Toll-like receptor triggering of a vitamin D-mediated human antimicrobial response. Science 311, 1770–1773.

Macedo, L.C., Soardi, F.C., Ananias, N., Belangero, V.M., Rigatto, S.Z., De-Mello, M.P., D'Souza-Li, L., 2008. Mutations in the vitamin D receptor gene in four patients with hereditary 1,25-dihydroxyvitamin D-resistant rickets. Arq. Bras. Endocrinol. Metabol. 52, 1244–1251.

Malloy, P.J., Eccleshall, T.R., Gross, C., Van Maldergem, L., Bouillon, R., Feldman, D., 1997. Hereditary vitamin D resistant rickets caused by a novel mutation in the vitamin D receptor that results in decreased affinity for hormone and cellular hyporesponsiveness. J. Clin. Invest. 99, 297–304.

Malloy, P.J., Zhu, W., Zhao, X.Y., Pehling, G.B., Feldman, D., 2001. A novel inborn error in the ligand-binding domain of the vitamin D receptor causes hereditary vitamin D-resistant rickets. Mol. Genet. Metab. 73, 138–148.

Malloy, P.J., Xu, R., Peng, L., Clark, P.A., Feldman, D., 2002. A novel mutation in helix 12 of the vitamin D receptor impairs coactivator interaction and causes hereditary 1,25-dihydroxyvitamin D-resistant rickets without alopecia. Mol. Endocrinol. 16, 2538–2546.

Malloy, P.J., Xu, R., Peng, L., Peleg, S., Al-Ashwal, A., Feldman, D., 2004. Hereditary 1,25-dihydroxyvitamin D resistant rickets due to a mutation causing multiple defects in vitamin D receptor function. Endocrinology 145, 5106–5114.

Malloy, P.J., Feldman, D., 2010. Molecular defects in the vitamin D receptor associated with hereditary 1,25-dihydroxyvitamin D-resistant rickets (HVDRR). In: Holick, M.F. (Ed.), Vitamin D: Physiology, Molecular Biology, and Clinical Applications. Humana Press (Springer Ed.), New York, pp. 691–714.

Malloy, P.J., Feldman, D., 2011. The role of vitamin D receptor mutations in the development of alopecia. Mol. Cell. Endocrinol. 347, 90–96.

Mangin, M., Sinha, R., Fincher, K., 2014. Inflammation and vitamin D: the infection connection. Inflamm. Res. 63, 803–819.

Miller, J., Djabali, K., Chen, T., Liu, Y., Ioffreda, M., Lyle, S., Christiano, A.M., Holick, M., Cotsarelis, G., 2001. Atrichia caused by mutations in the vitamin D receptor gene is a phenocopy of generalized atrichia caused by mutations in the hairless gene. J. Invest. Dermatol 117, 612–617.

Molnár, F., Peräkylä, M., Carlberg, C., 2006. Vitamin D receptor agonists specifically modulate the volume of the ligand-binding pocket. J. Biol. Chem. 281, 10516–10526.

Molnár, F., 2014. Structural considerations of vitamin D signaling. Front. Physiol. 5, 191.

Molnár, F., Sigueiro, R., Sato, Y., Araujo, C., Schuster, I., Antony, P., Peluso, J., Muller, C., Mourino, A., Moras, D., Rochel, N., 2011. 1α,25$(OH)_2$-3-epi-vitamin D_3, a natural physiological metabolite of vitamin D_3: its synthesis, biological activity and crystal structure with its receptor. PLoS One 6 e18124.

Morris, H.A., Anderson, P.H., 2010. Autocrine and paracrine actions of vitamin D. Clin. Biochem. Rev. 31, 129–138.

Nakabayashi, M., Tsukahara, Y., Iwasaki-Miyamoto, Y., Mihori-Shimazaki, M., Yamada, S., Inaba, S., Oda, M., Shimizu, M., Makishima, M., Tokiwa, H., Ikura, T., Ito, N., 2013. Crystal structures of hereditary vitamin D-resistant rickets-associated vitamin D receptor mutants R270L and W282R bound to 1,25-dihydroxyvitamin D_3 and synthetic ligands. J. Med. Chem. 56, 6745–6760.

Nguyen, T.M., Adiceam, P., Kottler, M.L., Guillozo, H., Rizk-Rabin, M., Brouillard, F., Lagier, P., Palix, C., Garnier, J.M., Garabedian, M., 2002. Tryptophan missense mutation in the ligand-binding domain of the vitamin D receptor causes severe resistance to 1,25-dihydroxyvitamin D. J. Bone Min. Res. 17, 1728–1737.

Nguyen, M., d'Alesio, A., Pascussi, J.M., Kumar, R., Griffin, M.D., Dong, X., Guillozo, H., Rizk-Rabin, M., Sinding, C., Bougnères, P., Jehan, F., Garabédian, M., 2006. Vitamin D-resistant rickets and type 1 diabetes in a child with compound heterozygous mutations of the vitamin D receptor (L263R and R391S): dissociated responses of the CYP-24 and rel-B promoters to 1,25-dihydroxyvitamin D_3. J. Bone Min. Res. 21, 886–894.

Nolte, R.T., Wisely, G.B., Westin, S., Cobb, J.E., Lambert, M.H., Kurokawa, R., Rosenfeld, M.G., Willson, T.M., Glass, C.K., Milburn, M.V., 1998. Ligand binding and co-activator assembly of the peroxisome proliferator-activated receptor-gamma. Nature 395, 137–143.

Norman, A.W., Bouillon, R., Farach-Carson, M.C., Bishop, J.E., Zhou, L.X., Nemere, I., Zhao, J., Muralidharan, K.R., Okamura, W.H., 1993. Demonstration that 1β,25-dihydroxyvitamin-D_3 is an antagonist of the nongenomic but not genomic biological responses and biological profile of the 3 a-ring diastereomers of 1α,25-dihydroxyvitamin-D_3. J. Biol. Chem. 268, 20022–20030.

Osz, J., Brélivet, Y., Peluso-Iltis, C., Cura, V., Eiler, S., Ruff, M., Bourguet, W., Rochel, N., Moras, D., 2012. Structural basis for a molecular allosteric control mechanism of cofactor binding to nuclear receptors. Proc. Natl. Acad. Sci. U. S. A. 109, E588–E594.

Orlov, I., Rochel, N., Moras, D., Klaholz, B.P., 2012. Structure of the full human RXR/VDR nuclear receptor heterodimer complex with its DR3 target DNA. EMBO J. 31, 291–300.

Otterbein, L.R., Cosio, C., Graceffa, P., Dominguez, R., 2002. Crystal structures of the vitamin D-binding protein and its complex with actin: structural basis of the actin-scavenger system. Proc. Natl. Acad. Sci. U. S. A. 99, 8003–8008.

Pike, J.W., 2011. Genome-wide principles of gene regulation by the vitamin D receptor and its activating ligand. Mol. Cell Endocrinol. 347, 3–10.

Ponchon, G., DeLuca, H.F., 1969. The role of the liver in the metabolism of vitamin D. J. Clin. Invest. 48, 1273–1279.

Prosser, D.E., Jones, G., 2004. Enzymes involved in the activation and inactivation of vitamin D. Trends biochem. Sci. 29, 664–673.

Reddy, G.S., Rao, D.S., Siu-Caldera, M.L., Astecker, N., Weiskopf, A., Vouros, P., Sasso, G.J., Manchand, P.S., Uskokovic, M.R., 2000. 1α,25-dihydroxy-16-ene-23-yne-vitamin D_3 and 1α,25-dihydroxy-16-ene-23-yne-20-epi-vitamin D_3: analogs of 1α,25-dihydroxyvitamin D_3 that resist metabolism through the C-24 oxidation pathway are metabolized through the C-3 epimerization pathway. Arch. Biochem. Biophys. 383, 197–205.

Rochel, N., Wurtz, J.M., Mitschler, A., Klaholz, B., Moras, D., 2000. The crystal structure of the nuclear receptor for vitamin D bound to its natural ligand. Mol. Cell 5, 173–179.

Rochel, N., Hourai, S., Moras, D., 2010. Crystal structure of hereditary vitamin D-resistant rickets–associated mutant H305Q of vitamin D nuclear receptor bound to its natural ligand. J. Steroid Biochem. Mol. Biol. 121, 84–87.

Rochel, N., Ciesielski, F., Godet, J., Moman, E., Roessle, M., Peluso-Iltis, C., Moulin, M., Haertlein, M., Callow, P., Mely, Y., Svergun, D.I., Moras, D., 2011. Common architecture of nuclear receptor heterodimers on DNA direct repeat elements with different spacings. Nat. Struct. Mol. Biol. 18, 564–570.

Shaffer, P.L., Gewirth, D.T., 2002. Structural basis of VDR-DNA interactions on direct repeat response elements. EMBO J. 21, 2242–2252.

Shiau, A.K., Barstad, D., Loria, P.M., Cheng, L., Kushner, P.J., Agard, D.A., Greene, G.L., 1998. The structural basis of estrogen receptor/coactivator recognition and the antagonism of this interaction by tamoxifen. Cell 95, 927–937.

Singarapu, K.K., Zhu, J., Tonelli, M., Rao, H., Assadi-Porter, F.M., Westler, W.M., DeLuca, H.F., Markley, J.L., 2011. Ligand-specific structural changes in the vitamin D receptor in solution. Biochemistry 50, 11025–11033.

Strushkevich, N., Usanov, S.A., Plotnikov, A.N., Jones, G., Park, H.W., 2008. Structural analysis of CYP2R1 in complex with vitamin D_3. J. Mol. Biol. 380, 95–106.

van Driel, M., Koedam, M., Buurman, C.J., Roelse, M., Weyts, F., Chiba, H., Uitterlinden, A.G., Pols, H.A.P., van Leeuwen, J.P.T.M., 2006. Evidence that both 1α,25-dihydroxyvitamin D_3 and 24-hydroxylated D_3 enhance human osteoblast differentiation and mineralization. J. Cell. Biochem. 99, 922–935.

Vanhooke, J.L., Benning, M.M., Bauer, C.B., Pike, J.W., DeLuca, H.F., 2004. Molecular structure of the rat vitamin D receptor ligand binding domain complexed with 2-carbon-substituted vitamin D_3 hormone analogues and a LXXLL-containing coactivator peptide. Biochemistry 43, 4101–4110.

Verboven, C., Rabijns, A., De Maeyer, M., Van Baelen, H., Bouillon, R., De Ranter, C., 2002. A structural basis for the unique binding features of the human vitamin D-binding protein. Nat. Struct. Biol. 9, 131–136.

Whitfield, G.K., Selznick, S.H., Haussler, C.A., Hsieh, J.C., Galligan, M.A., Jurutka, P.W., Thompson, P.D., Lee, S.M., Zerwekh, J.E., Haussler, M.R., 1996. Vitamin D receptors from patients with resistance to 1,25-dihydroxyvitamin D_3: point mutations confer reduced transactivation in response to ligand and impaired interaction with the retinoid X receptor heterodimeric partner. Mol. Endocrinol. 10, 1617–1631.

Please cite this article in press as: Rochel, N., Molnár, F., Structural aspects of Vitamin D endocrinology, Molecular and Cellular Endocrinology (2017), http://dx.doi.org/10.1016/j.mce.2017.02.046

Yamada, S., Makishima, M., 2014. Structure-activity relationship of nonsecosteroidal vitamin D receptor modulators. Trends Pharmacol. Sci. 35, 324–337.
Zhang, J., Chalmers, M.J., Stayrook, K.R., Burris, L.L., Garcia-Ordonez, R.D., Pascal, B.D., Burris, T.P., Dodge, J.A., Griffin, P.R., 2010. Hydrogen/deuterium exchange reveals distinct agonist/partial agonist receptor dynamics within vitamin D receptor/retinoid X receptor heterodimer. Structure 18, 1332–1341.
Zhang, J., Chalmers, M.J., Stayrook, K.R., Burris, L.L., Wang, Y., Busby, S.A., Pascal, B.D., Garcia-Ordonez, R.D., Bruning, J.B., Istrate, M.A., Kojetin, D.J., Dodge, J.A., Burris, T.P., Griffin, P.R., 2011. DNA binding alters coactivator interaction surfaces of the intact VDR-RXR complex. Nat. Struct. Mol. Biol. 18, 556–563.
Zhou, Y., Wang, J., Malloy, P.J., Dolezel, Z., Feldman, D., 2009. Compound heterozygous mutations in the vitamin D receptor in a patient with hereditary 1,25-dihydroxyvitamin D-resistant rickets with alopecia. J. Bone Min. Res. 24, 643–651.
Zou, J., Minasyan, A., Keisala, T., Zhang, Y., Wang, J.H., Lou, Y.R., Kalueff, A., Pyykkö, I., Tuohimaa, P., 2008. Progressive hearing loss in mice with a mutated vitamin D receptor gene. Audiol. Neurootol 13, 219–230.

Please cite this article in press as: Rochel, N., Molnár, F., Structural aspects of Vitamin D endocrinology, Molecular and Cellular Endocrinology (2017), http://dx.doi.org/10.1016/j.mce.2017.02.046